Supplementary Information

Functional rewiring across spinal injuries via biomimetic nanofiber scaffolds

Sadaf Usmani, Audrey Franceschi Biagioni, Manuela Medelin, Denis Scaini, Raffaele Casani, Emily R. Aurand, Daniel Padro, Ander Egimendia, Pedro Ramos Cabrer, Manuela Scarselli, Maurizio De Crescenzi, Maurizio Prato* and Laura Ballerini*

Correspondence to: Laura Ballerini laura.ballerini@sissa.it; Maurizio Prato prato@units.it

Materials and Methods

Preparation of implants

Three-dimensional multi-walled carbon nanotubes (MWCNTs) were obtained from Prof. Maurizio De Crescenzi's laboratory[1,2]. As previously reported[3], this MWCNT-scaffold (CNF) is a free-standing three-dimensional framework of self-assembled MWCNTs. The interconnected MWCNTs are characterized by high electrical conductivity, by the ability to be compressed without structure deformation and by stiffness values (Young's modulus) within the order of the human CNS tissue (0.1 kPa-20 kPa)[4]. For the implant, sharp pointed cylinders (1.79±0.37 mm length and 0.76 ± 0.11 mm in diameter, confirmed by MRI) were carved out under visual control (dissection microscopy) with a scalpel blade from the larger 3D scaffold bulk material. The material stiffness was increased to provide a transient structural support to the CNF in order to facilitate handling and implantation in the spinal lesion. This was achieved by embedding the material into commonly used polymer: PEG-4000 (Poly (ethylene glycol,100%); 81240 from Sigma Aldrich, average MW 4,000 Da;[3] at 65 °C and then leaving it to solidify by cooling at room temperature (20-22 °C, RT). PEG-alone implants were prepared in a similar fashion and with matching dimensions but without the inclusion of CNF. PEG or

www.pnas.org/cgi/doi/10.1073/pnas.2005708117

PEG-CNF scaffolds were further attached to a glass capillary to allow ease of implantation during surgery.

Surgical procedures and animal care

All procedures, housing and post-operative care were approved by the Italian Ministry of health; authorization #938/2015-PR and behavior of rats was monitored regularly under the supervision of the institution's authorized veterinarian and the institutional ethical committee.

Fifty-eight adult female Wistar rats (age 2-3 months) were recruited for lumbar spinal hemisection model; 17 animals were allocated to the PEG control group (6 lesion with no implant and 11 PEG implanted; these animals were pooled together since no differences were observed in histological, MRI and behavioral analysis; regarding their locomotor performance and histology see supplementary Fig. S3 A-C), and 28 animals were assigned to the test CNF (CNF-implanted) group. In setting the lesion model, we used 5 additional animals (sacrificed 24 hours after-surgery) to check the lesion size correlation to the (BBB) locomotor performance (supplementary Fig. S3 D).

Four additional animals with lumbar spinal hemisection and 2 healthy controls were injected with neuro-tracer for tract tracing experiments (see below) and 2 healthy control was used for MRI analysis (see below).

Unilateral L1-L2 spinal hemisection model was utilized to produce a partial spinal-cord lesion[5]. Briefly, animals were anaesthetized with Ketamine (80 mg/kg) and Xylazine (10 mg/kg) i.p. and the spinal-cord was exposed using a dissecting microscope by drilling a hole in the lamina of T13 vertebra[5]. A 3 mm diameter wide hole/window was drilled into the right lamina to approach the spinal-cord and by surgical blade a small incision of the

dura was made followed by durotomy[5]. A lateral hemisection (hemicordectomy) at the L1 level on the right side of the spinal-cord was achieved by creating a 2 mm-long longitudinal lesion using micro-scissors (7 mm fine tip) making two mediolateral incisions along the midline towards the rostral and caudal end of the hole/window and the tissue was removed by sharp forceps. This created a lesion of 2 mm in length. An independent observer confirmed the adequacy of the acute lesion length and size. Hemostasis was achieved by using absorbable hemostatic gelatin sponge (Spongostan-Dental; Ferrosan). The treatments, when consisting of the insertion of the CNF embedded in PEG or the PEG implants, were administered blindly to the lesion. A group of animals with the hemisection alone were initially used as controls (see above). Surgeries were performed in a randomized manner and the two, PEG and CNF, or three, lesion alone, PEG and CNF, groups were performed on the same day to minimize differences or surgical bias among groups. The skin was closed using surgical staples (Tweek Vistat 35R). Throughout the whole procedure, respiration, body temperature, heart rate and oxygen saturation were regularly monitored[6] to assess the depth of anesthesia and animal well-being. Animals were checked at regular intervals for the first 72 hours post-surgery. All groups were administered prophylactic antibiotic (Baytril–Enrofloxacin; 5 mg/kg, intraperitoneal) and analgesic solution (Rymadyl; 5 mg/kg, intraperitoneal) immediately after the surgery and for 3 consecutive days post-surgery. All animals used in the study showed no sign of pain or distress, following 72 hours period, animals were monitored once per day until sacrifice.

Immunohistochemistry, image acquisition, confocal microscopy and analysis

Upon perfusion spinal-cords were carefully dissected, post fixed in 4 % formaldehyde (prepared from fresh paraformaldehyde) in PBS for 24 hours at 4 °C, and cryprotected in 30 % sucrose in PBS at 4 °C until they sunk in the solution. Cryoprotected spinal-cords were then quick-frozen in optimal cutting temperature compound (Tissue-Tek), frozen at – 20 °C, and cryosectioned into 30 µm thick longitudinal sections by using a cryostat (Microm HM 550, Thermo Fisher Scientific). Tissue-Tek was washed by PBS and tissue sections were incubated for 5 min in glycine 0.1 M, blocked in 3 % BSA (Sigma), 3 % FBS (Gibco) or 3% NGS (Abcam), 0.3 % Triton X-100 (Carlo Erba) in PBS for 45 min at RT and then incubated overnight at 4 °C with primary antibodies (mouse anti-GFAP, 1:400, Sigma; rabbit anti-Iba1, 1:500, Wako; rabbit anti-β-tubulin III, 1:500, mouse anti-RECA1 1:250, Bionova) in 5 % FBS in PBS. Following washing in PBS, sections were incubated for 2 h at room temperature in secondary antibodies (goat anti-rabbit Alexa 594, 1:400, Invitrogen; goat anti-mouse Alexa 488, 1:400, Invitrogen; DAPI, 1:500, Invitrogen) in 5 % FBS in PBS.

In order to identify the type of regenerating axons, CNF slices were further processed for immunofluorescence with (primary antibodies): rabbit anti-5-HT (1:1000, Sigma), guinea-pig anti-VGLUT1 (1:2000, Millipore), and rabbit or mouse anti-β-tubulin III (1:500) in 5 % FBS in PBS incubated overnight at 4 °C. Following washing in PBS, sections were incubated for 2 h at room temperature in secondary antibodies (goat anti-rabbit or goat-anti mouse Alexa Fluor 405, 1:300, or 488, 1:400, Invitrogen; goat anti-guinea-pig Alexa Fluor 488, 1:400, Invitrogen; goat anti-rabbit Alexa Fluor 594) in 5 % FBS in PBS.

Tissue sections were then mounted on glass coverslips using Vectashield hard mounting medium (Vector Laboratories) or Fluoromount G (Invitrogen). The lesion area was measured from immunolabeled slices (≥ 5 slices each spinal-cord) at 2 (n = 5 and 5, PEG and CNF), 4 (n = 5 and 7, PEG and CNF) and 6 (n = 5 and 4, PEG and CNF) months post-surgery by using FIJI software[7]. As no data differences were detected among subsequent time points within each group, results were pooled together. Quantification of tissue reaction was achieved by measuring GFAP and Iba1 labelling. Fluorescence images were acquired using a Leica DM6000 upright microscope with a 10× (n.a. 0.3) dry objective. Identical binning, gains and exposure times were used for all images of the same marker. Image analysis was performed using the FIJI software. For both GFAP and Iba1 analysis, in each 30 µm mounted section n = 6 region of interest (ROIs; 100 × 500 μm^2) were selected at fixed distances from the lesion edge (both rostrally and caudally): 0 µm, 100 µm and 500 µm). The background intensity threshold was defined for each spinal-cord section using the labeling intensity measured in the contralateral spinal-cord (left side) at 500 µm rostral and caudal from the contralateral lesion edge. The area within each ROI with intensity above the background threshold was calculated, normalized to the contralateral hemicord and used for statistics. Therefore, for each subject (not subjected to further tissue processing, immunolabeling or neurotracing), data are presented as arbitrary units (a.u.), representing the fold increase of both GFAP and Iba1 over baseline levels estimated in the contralateral uninjured cord.

Quantification of β-tubulin III and RECA positive signals within the lesion area was done by acquiring confocal images at 40× (n.a., 0.95) with a Nikon A1R confocal microscope,

equipped with solid state lasers. We computed positive signals detected within the CNF implant and reaching the epicenter of the implanted CNF from confocal images selecting five ROIs from each slice, one at the epicenter and the remaining four as projections of 45° diagonal lines from the center to the edge of the implant (Supplementary Fig. S2). β-tubulin III positive fibers were computed if displaying ≥ 20 μm length. The percentage of fields within the implant or at the epicenter where β-tubulin III-positive and RECA-positive vascular structures were detected was calculated. The presence of neuronal cell body within the scaffold was tested by NeuN-nuclear neuronal labeling (Fig.S2) of tissue sections (n=14 sections from 2 CNF animals at 6 months from implantation) with (primary antibody) mouse anti-NeuN (1:100; Merck Millipore) prepared in 5% NGS (in PBS) incubated overnight at 4 ^{o}C. Following washing, 2 hours incubation at room temperature with (secondary antibody) goat anti-rabbit Alexa Fluor 488, (1:400, Invitrogen) in 5% NGS (in PBS).

In order to visualize the CNF 3D-structure the reflection mode[3] setting available in the Nikon A1R microscope was utilized. Raw z-were transformed into 8-bit and saved as STL surface file using 3D_viewer plugin in FIJI. STL file was transformed in 3D object and displayed using the Open source software Blender V2.81.

Confocal microscopy images were acquired at the following magnifications: 10× (n.a., 0.45), 20× (n.a., 0.75), 40× (n.a., 0.95), 60× (n.a., 1.40) 100× (n.a., 1.45).

Scanning Electron microscopy (SEM)

CNF morphology was qualitatively assessed through SEM in CNF alone and in PFA fixed longitudinal 30 μm sections of the CNF spinal-cord. Images were acquired

collecting secondary electrons on a Gemini SUPRA 40 SEM (Carl Zeiss NTS GmbH). Before imaging, a metal sputter coater was used to gold-metalize the sample.

Finite element simulation (FEM) of the spinal cord

The qualitative spinal cord model used consisted of a cylindrical object 20 mm in length and 2 mm in diameter. The spinal cord was simplified to an isotropic and homogenous viscoelastic material, with identical properties assigned to grey and white matter. The viscoelastic portion of the material law was described with a two elements Prony series exponential decay. All the parameters used in the simulation are representative of murine spinal cord mechanical properties[8] and are summarized in the following Table:

v	**G_0**	**G_∞**	**g**	**τ**
0.45	188.2 kPa	32 kPa	g_1=0.5282	τ_1= 8 ms
			g_2=0.3018	τ_2= 150 ms

Two experimental conditions of SCI lesion were simulated: upon dissolution of the PEG insert, and upon placing a CNF insert with the same dimension of the removed tissue. The CNF insert is independent (not bound) from the rest of the spinal cord but was set to match its mechanical properties (see Table). In both conditions the lesion was modelled by the hemisection of the cylinder at central axial position with an edge radius of ~0.5 mm (see Fig.1F). The cylinder was constrained to a reference plane on its left facet while a uniform pressure is applied on the free right one (30 kPa). In order to simulate a condition of axial load on the spinal cord of a free-moving mouse a cylindrical constrain was set on the model to allow only sliding and contraction of the spinal cord. This condition is mimicking as well the restrain from vertebral bones.

The solid was modelled, carved and formed into solids. Subsequently was portioned into subregions for optimized mesh generation. The lesioned site of the spinal cord was meshed with a finer mesh seed when compared to the two ends. The implanted insert has an independent mesh set with common boundaries with the simulated spinal cord and same cylindrical constrains in order to maintain overall continuity. The simulation evaluated the absolute deformation in terms of displacement (in mm) and the von Mises stress (in kPa). Pre- and post-processing were performed on a PC workstation using SolidWorks 3D CAD package (Dassault Systèmes SE, FR), and FEM simulations were performed using SW simulation module on a workstation equipped with a 4-cores Intel i7 processor and 16 GB of RAM running Windows 10 Professional Edition.

Magnetic Resonance Imaging

Magnetic Resonance Imaging studies were conducted at 11.7 Tesla using a Bruker Biospec USR 117/16 MRI system (Bruker Biospin GmbH, Ettlingen, Germany) with actively shielded gradients of 750 mT/m power and a slew rate of 6660 T/m/s. RF transmission was achieved by using a quadratic transmit volumetric coil of 72 mm of internal diameter (Bruker T1148V3), and RF reception was achieved with a surface coil (Bruker T11657V3) of □2 cm of diameter.

Excised vertebral columns with surrounding muscle tissue were imbibed in 50 ml Falcon tubes containing 1% (w/v) low EEO agarose gels (Sigma-Aldrich, CAS: 9012-36-6) for fixation. Falcon tubes were firmly attached to the MRI receive coil with tape, taking special care to place the L1 vertebra at the center of the coil (in order to achieve maximal signal to noise ratio at the region of interest).

Three sets of multi-slice low resolution images were acquired for reference (scout images: FLASH -fast low angle shot- image sequence with fat suppression, echo time TE=2.5 ms, Repetition time TR=200 ms, $N_{averages}$ = 4, Flip angle 40 degrees, Field of view 60 × 30 matrix of 256 × 128 points and 32 slices of 0.5 mm thickness (sagittal or coronal orientation) or 32 × 32 mm, matrix of 128 × 128 points and 24 slices of 0.5 mm thickness (axial orientation), and a bandwidth of 150 kHz. Finally 2 sets of high resolution DTI – diffusion weighted imaging- Images were acquired using the following parameters: Set 1) Spin-echo DTI pulse sequence, echo time TE = 20.3 ms, δ = 4 ms, Δ = 11 ms, b = 1000 mm^{-2} s, 30 directions + 5 b0 images, Repetition time TR = 2127.7 ms, Averages = 1, Axial orientation, field of view FOV= 25.6 × 25.6 mm, matrix of 256 × 256 points, 32 consecutive slices of 0.5 mm thickness, bandwidth 66 kHz, scan time = 3h 59m. Set 2) Spin-echo DTI pulse sequence, echo time TE = 21.5 ms, δ = 4.5 ms, Δ = 11 ms, b = 750 mm-2 s, 30 directions + 5 b0 images, Repetition time TR= 1418.44 ms, Averages = 4, Axial orientation, field of view FOV = 25.6 × 25.6 mm, matrix of 256 × 256 points, 48 consecutive slices of 0.25 mm thickness, bandwidth 120 kHz, scan time = 11h 22m.

The open source software DIPY (Diffusion Imaging in python)[9] with local PCA denoising[10], was used for the processing of acquired DTI images, to obtain fractional anisotropy (FA), mean diffusivity (MD), Radial Diffusivity (RA) and Axial diffusivity (AD) maps. Measuring by DWI the diffusion coefficients of water molecules at different directions in space allows calculating the Fractional Anisotropy (FA; range from 0 to 1). CNS regions containing white matter (WM) display elevated FA values (FA > 0.8 and FA > 0.6 for in vivo and ex vivo spinal cord WM in the rat[11], while CSF is characterized

by FA values < 0.1 and CNS grey matter has intermediate-to-low FA values (FA < 0.4, in vivo, or FA < 0.3, ex vivo, for spinal cord grey matter[11]. Image processing and quantification of parameters in selected regions of interest has been performed with Image-J software, from NIH. Finally, fiber tracking analysis has been performed with the med-Inria software (V3.0)[12], using the Tensor estimation algorithm with no masking algorithm and the TTK tensor algorithm for fiber tracking calculations with a starting and stopping FA threshold of 0.3 and a minimum fiber length of 1 mm. Quantification of fibers in regions of interest was achieved with the software DTIstudio 2.4 using a starting and stopping FA threshold of 0.35 fiber tracking calculations.

The MRI analysis and quantifications of fibers was performed in the entire spinal cord due to the small size of the rat spinal cord and the spatial resolution achieved in acquired DTI images.

Representation of fiber tracks through the spinal cord were constructed from DTI data using MedInria 3.0 software[13]. After loading DTI data, diffusion tensors where calculated using TTK tensor estimation algorithm without DWI masking and no smoothing. Then fiber tracks were constructed using the TTK tractography algorithm using starting and stopping Fractional Anisotropy threshold values of 300 and 150, zero value for smoothness and for minimum fiber length and a sampling factor of 1. Fibers were displayed as tubes with local orientation color LUT. Bundling box option has been used to display fibers of one half of the spine, to facilitate visualization.

Dextran tracing

Dextran, Alexa FluorTM 594 (10,000 MW, Anionic, Fixable; Thermo Fisher Scientific; 10 % wt/ vol solution) was microinjected (1 µL; 0.1 µL per minute) at two points in the

sensory motor cortex contralateral to the side of the spinal-cord hemisection at 3 months post-surgery. For injections we used the following coordinates anterior–posterior (AP), 1.44 mm; medial–lateral (ML), 2 mm; dorsal–ventral (DV), -2.4 mm; AP, -0.96 mm; ML, 4 mm; DV, -2.6 mm to target the motor and sensory cortex, using bregma as the reference[14]. Four weeks later, rats were sacrificed, following cryosectioning of the tissue, slices were mounted on positively charged glass slides and washed once with PBS (0.1 M). All sections were mounted with Fluoromount (Sigma, USA) and visualized using the confocal microscope (Nikon A1 R) acquired with 4×, 40× (dry) and 60× 100× oil objective (n.a. 1.2) using oil-mounting medium (1.515 refractive index) and analyzed using *ImageJ* software.

Behavioral studies

Open field observation of hindlimb locomotor recovery was assessed by using the Basso-Beattie-Bresnahan (BBB) rating scale[15]. BBB score of zero represents no hind limb movement while the highest score of 21 represents stable walking. This scale takes into consideration behavior from individual joint movements of the hindlimb, to plantar stepping, to coordinated walking and finally the subtler behaviors of locomotion, such as paw position, trunk stability and tail position. Each animal was tested individually in an open field (80 cm × 80 cm), at the same time each day, video recorded and graded by the same blinded observers. No training was essential for BBB locomotor rating. Animals were habituated to their surroundings and the open field at pretesting stage to reduce their anxiety levels.

We specifically tested the relationship between lesion dimension (area) and 24 hours post-surgery BBB score to validate both our scoring method and the surgery control of

the initial lesion, which was done on purpose of increasing dimensions. Such results are described in supplementary Fig. S3 B.

Skilled sensory-motor behavior was assessed by the ladder beam test[16,17] by grading stepping, limb placing and motor control on each rung, on a scale from 0 to 5. Scoring was characterized as drag, miss, deep slip, slight slip, partial placement, and a correct placement respectively, where zero represents a drag and a five represents a correct paw placement[16,17]. Sum of scores recorded in the same session were further normalized with number of steps / limb placements and the baseline score (recorded prior to SCI) to ensure accuracy and inter-animal comparison. Hence the formula to calculate grading for each session was as follows:

(sum of scores obtained from all steps or limb placements)/ (number of steps or limb placements)(baseline score)*

Rats were made, at the same time each day, to pass twice a one-meter-long horizontal ladder beam with equally spaced rungs; they were video recorded and graded offline by the same blinded observers. All rats were trained for 7 consecutive days prior to the surgery to pass the ladder with all correct placements. The strength of the ladder rung test is that it provides more descriptive accounts on impairment. To perform tasks on the ladder, animals need regular limb coordination and control weight support to correctly place limbs.

Walking stability, onset of plantar placement and inter-limb coordination was assessed by footprint analysis[18]. For collection of footprints, forepaws and hind paws were painted with different colors and rats were encouraged to walk in a straight line along a meter-long reward-directed runway over absorbent paper. A series of at least five consecutive

steps were used to determine the mean values of each measurement. Since the aim of this task is to assess spontaneous walking pattern, no training was required. Baseline recording was taken 24 hours before surgery.

Data analysis, statistics and reproducibility

All values from samples subjected to the same experimental protocols were pooled together and expressed as mean ± SE, unless otherwise indicated, with n = biologically independent experiments, usually number of animals, unless otherwise indicated. Levene's or D'Agostini's test was used to assess the homogeneity of variances. Statistically significant difference between two data sets was assessed by one-tailed Student's t-test for parametric data and by Mann–Whitney for non-parametric ones. Statistical significance between two parametric data sets was identified by Student's t-test. P-value between lesion areas of PEG and CNF groups was = 0.001. FA values representing white matter within CNF was significantly higher than in PEG implanted rats (P = 1.93 E-05).

Student's t-test showed a significant increase in the sub-acute ($P \leq 0.05$; on day 1, 2, 3 and 5) and sub-chronic phases ($P \leq 0.05$ on day 22, 29 and at 2, 3 and 4 months) in the BBB testing.

Motor ability measured by the ladder-beam test was improved by the CNF implantation in a sub- acute ($P < 0.01$ on day 1, 5 and 7; $P \leq 0.001$ on day 2, 3, 10) and sub-chronic phase ($P \leq 0.01$ on day 15, 22 and $P < 0.05$ on day 29). Statistical significance was determined at $P < 0.05$. Significance was graphically indicated as follows: *P < 0.05, **P < 0.01, ***P < 0.001.

In box plots, the thick horizontal bar indicates the median value, while the boxed area extends from the 25th to 75th percentiles with the whiskers ranging from the 5th to the 95th percentiles.

SI Appendix References

1. L. Camilli *et al.*, Pressure-dependent electrical conductivity of freestanding three-dimensional carbon nanotube network. *Appl. Phys. Lett.* **102**, 183117 (2013).
2. L. Camilli, *et al.*, A three-dimensional carbon nanotube network for water treatment. *Nanotechonology*. **25**, 065701 (2014).
3. S. Usmani *et al.*, 3D meshes of carbon nanotubes guide functional reconnection of segregated spinal explants. *Sci. Adv.* **2**, e1600087 (2016).
4. Tyler, W. J. The mechanobiology of brain function. *Nat. Rev. Neurosci.* **13**, 867–878 (2012).
5. A. Roozbehi *et al.*, Age-associated changes on axonal regeneration and functional outcome after spinal cord injury in rats. *Acta Med. Iran* **53**, 281–286 (2015).
6. S. Marchesan, L. Ballerini, M. Prato, Nanomaterials for stimulating nerve growth. *Science* **356**, 1010–1011 (2017).
7. Fan, H. et al. Reactive astrocytes undergo M1 microglia/ macrophages-induced necroptosis in spinal cord injury. *Mol. Neurodegen.* **11,** 14 (2016).
8. J. T. Maikos, Z. Qian, D. Metaxas, D. I. Shreiber, Finite element analysis of spinal cord injury in the rat. *J. Neurotrauma* **25**, 795-816 (2008).

9. Garyfallidis, E. et al. Dipy, a library for the analysis of diffusion MRI data. *Front. Neuroinform.* **8**, 1–17 (2014).

10. Manjón, J. V. et al. Diffusion Weighted Image Denoising Using Overcomplete Local PCA. *PLoS One*. **8**, 1–12 (2013).

11. S. Madi, K. M. Hasan, P. A. Narayana, Diffusion tensor imaging of in vivo and excised rat spinal cord at 7 T with an icosahedral encoding scheme. *Magn. Reson. Med.* **53**, 118–125 (2005).

12. Fillard, P. & Toussaint, N. Medical Image Navigation and Research Tool by INRIA (MedINRIA). *Enseignement*, 1–39 (2006).

13. F. Vichot *et al.*, Cardiac Interventional Guidance using Multimodal Data Processing and Visualisation: medInria as an Interoperability Platform. *Midas Journal* http://hdl.handle.net/10380/3361(2012).

14. Paxinos, G. & Watson, C. R. *The Rat Brain in Stereotaxic Coordinates* (Elsevier Academic Press, San Diego, ed. 6th, 2007).

15. D. M. Basso, M. S. Beattie, J. C. Bresnahan, A Sensitive and Reliable Locomotor Rating Scale for Open Field Testing in Rats. *J. Neurotrauma* **12**, 1–21 (1995).

16. G. A. Metz, I. Q. Whishaw, The ladder rung walking task: A scoring system and its practical application. *J. Vis. Exp.* **28**, 1204 (2009).

17. Metz, G. A. & Whishaw, I. Q. Cortical and subcortical lesions impair skilled walking in the ladder rung walking test: a new task to evaluate fore- and hindlimb stepping, placing, and co-ordination. *J. Neurosci. Methods*. **115**, 169–179 (2002).

18. Scali, M. et al. Fluoxetine treatment promotes functional recovery in a rat model of cervical spinal cord injury. *Sci. Rep.* **3**, 2–7 (2013).

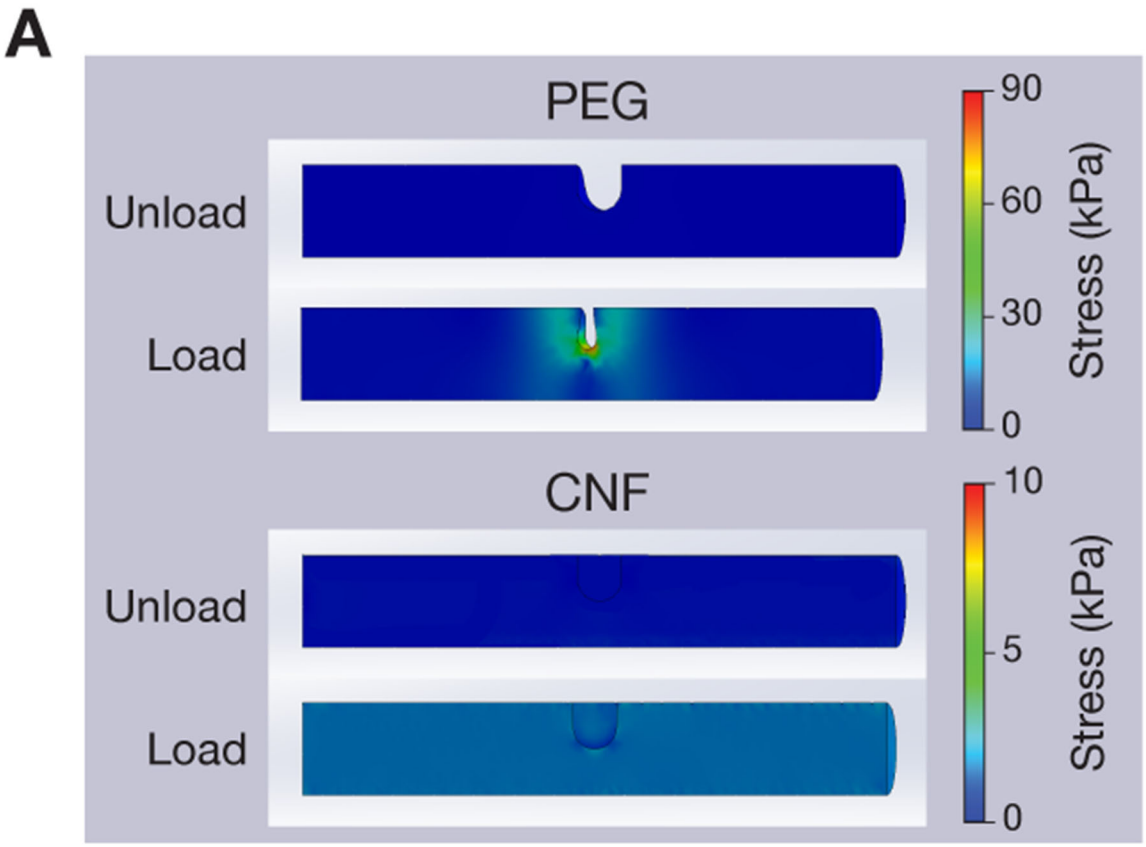

Fig. S1. (A) FEM simulation of a viscoelastic cylinder mimicking a lesioned spinal cord. Von Mises stress is color-coded and superimposed to the deformed images. Top: load and unload conditions when the SCI lesion is left empty after PEG dissolution (PEG). Bottom: load and unload conditions when in the SCI lesion an implant characterised by mechanical properties matching CNF ones is present (CNF).

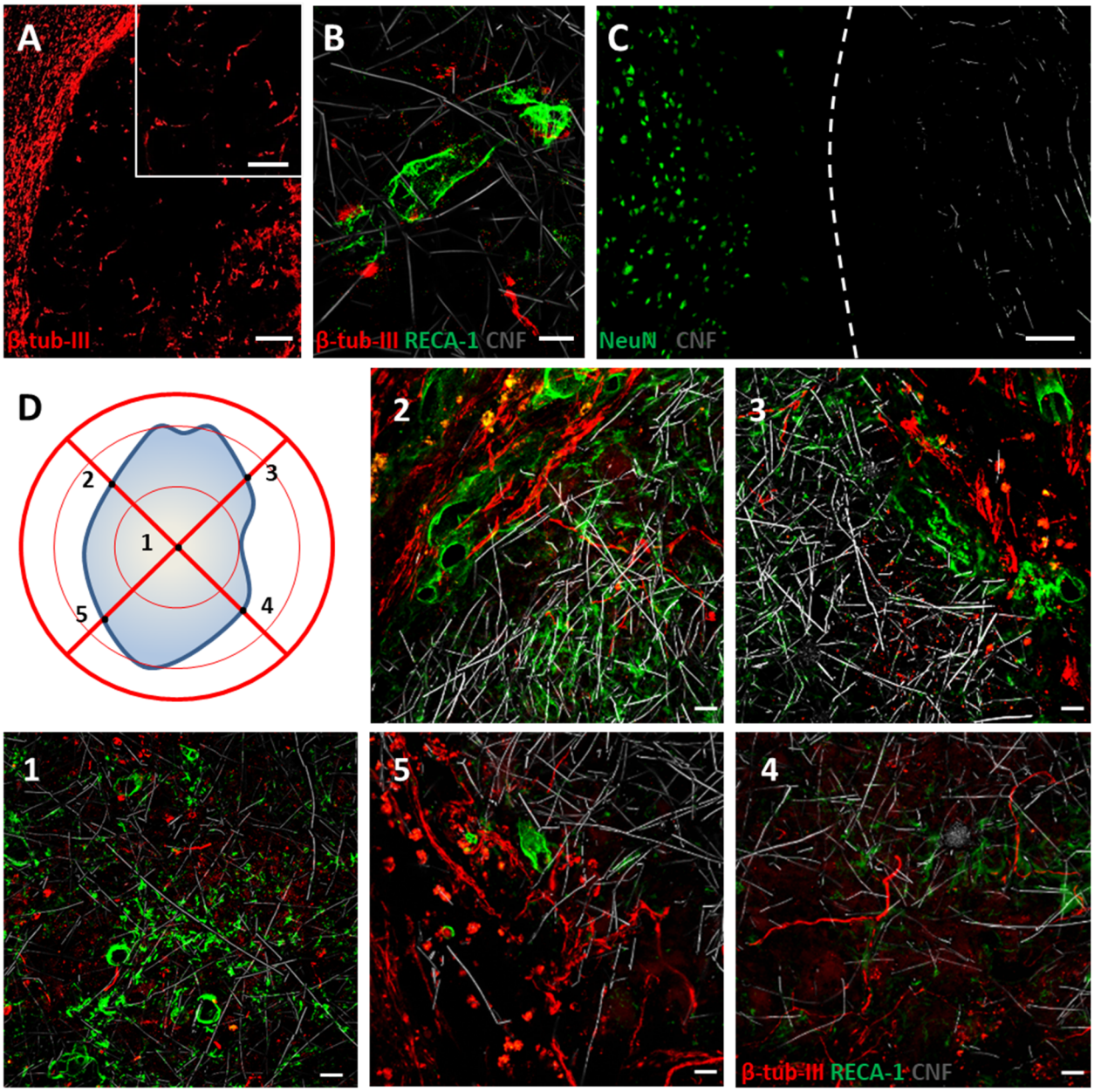

Fig. S2. (A) Low magnification confocal microscopy of β-tubulin III positive signals (in red) in SCI within the CNF implant and (inset) the corresponding higher magnification. (B) High magnification confocal micrograph of β-tubulin III and RECA positive signals (in green) identifying blood vessels and neurites within the CNF (in grey). (C) NeuN positive labelling (in green) is located in the intact spinal tissue contralateral to the CNF (in grey; the lesion border is highlighted by the dashed line). Note that NeuN positive cells were identified in the intact spinal tissue contralateral to the implanted lesion area, no NeuN positive neuronal nuclei were found inside the CNF scaffold. (D) Diagram of the fixed region of interest (ROI) acquired within the implant. Black dots at the intersection were taken as the center of each ROI. Additional ROI at the center of the implant was considered as the epicenter. Numbered micrographs are representative

confocal images corresponding to each ROIs. Presence of β-tubulin III and RECA positive structures were exploited for percentage quantification of implanted CNF containing neurites and blood vessels. All images at 6 months after-surgery. Scale bars: A (and inset) 100 μm; B 10 μm; C 100 μm; D 20 μm.

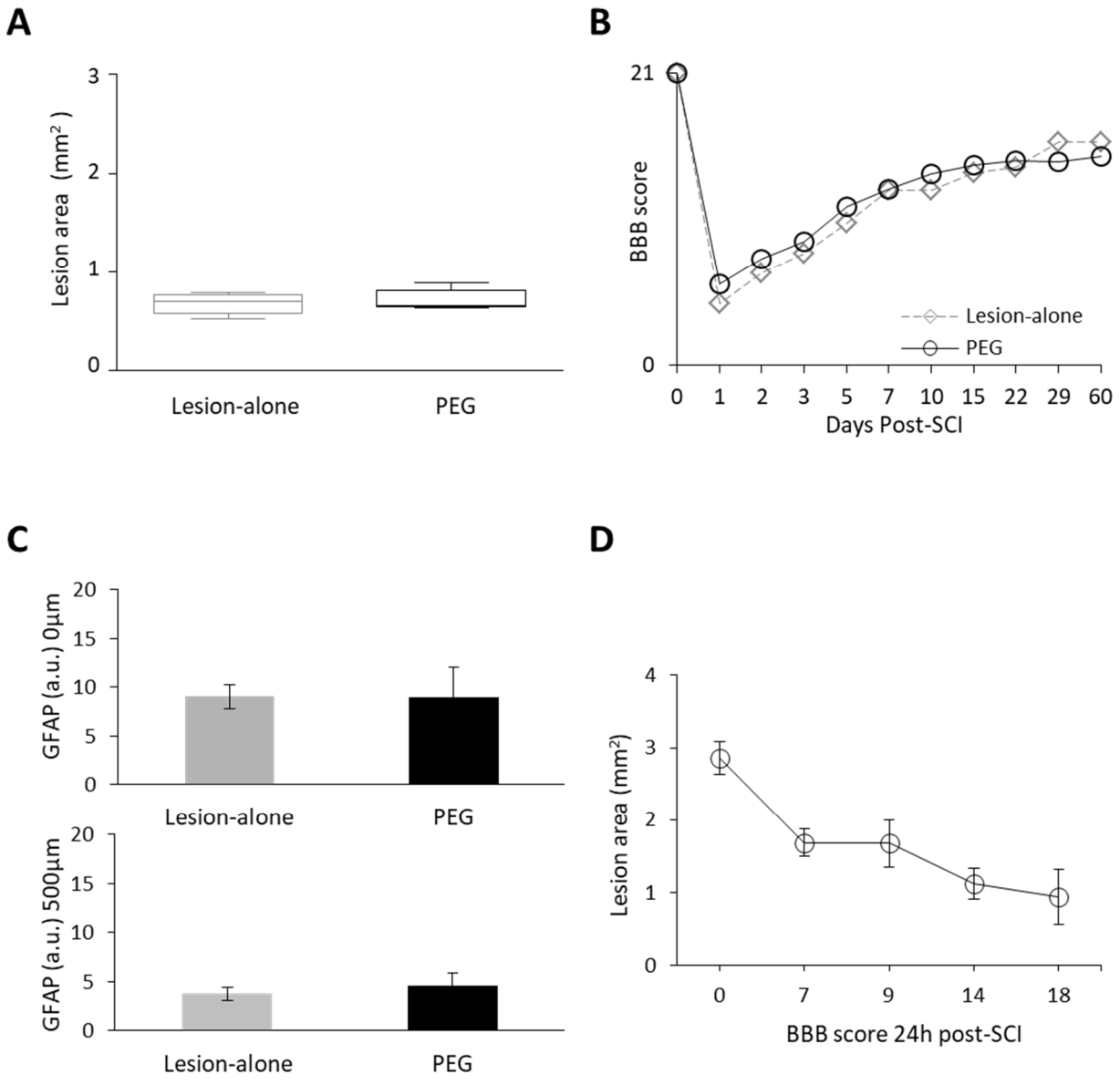

Fig. S3. (A) Box plot of the lesion dimension (n=5 each group), (B) BBB score and (C) GFAP intensity average values (top plot, measured at the lesion border, i.e. 0 μm;

bottom plot, measured at 500 μm distance from the lesion) separating “Lesion-alone” and “PEG” SCI control animals for direct comparison. No differences between “Lesion-alone” and PEG were found. (D) Correlation of lesion area with BBB score at 24 hours.

Movie M1. Confocal (reflection mode) 3D reconstructions of CNF scaffold.